

See discussions, stats, and author profiles for this publication at: <https://www.researchgate.net/publication/322507484>

# A Highly Sensitive Ratiometric Self-Assembled Micellar Nanoprobe for Nitroxyl and Its Application In Vivo

**Article** in *Analytical Chemistry* · January 2018

DOI: 10.1021/acs.analchem.7b04787

CITATIONS

0

**11 authors**, including:



**Feiyi Wang**

Hubei University

**19** PUBLICATIONS **469** CITATIONS

[SEE PROFILE](#)



**Junqi Nie**

Hubei University

**21** PUBLICATIONS **68** CITATIONS

[SEE PROFILE](#)

READS

44



**Cuifen Lu**

Hubei University

**50** PUBLICATIONS **328** CITATIONS

[SEE PROFILE](#)



**Qi Sun**

Wuhan Institute of Technology

**11** PUBLICATIONS **146** CITATIONS

[SEE PROFILE](#)

**Some of the authors of this publication are also working on these related projects:**



Fluorescence probe [View project](#)

# Highly Sensitive Ratiometric Self-Assembled Micellar Nanoprobe for Nitroxyl and Its Application In Vivo

Shaohua Yuan,<sup>†</sup> Feiyi Wang,<sup>\*,†,‡</sup> Guichun Yang,<sup>†</sup> Cuifen Lu,<sup>†</sup> Junqi Nie,<sup>†</sup> Zuxing Chen,<sup>†</sup> Jun Ren,<sup>†</sup> Yuan Qiu,<sup>‡</sup> Qi Sun,<sup>\*,‡</sup> Chunchang Zhao,<sup>\*,§</sup> and Wei-Hong Zhu<sup>§</sup>

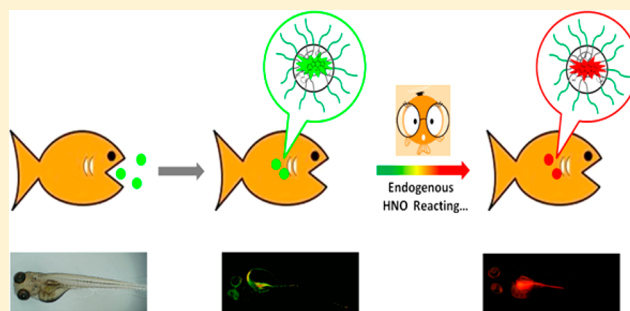
<sup>†</sup>Ministry of Education Key Laboratory for the Synthesis and Application of Organic Functional Molecules & Hubei Collaborative Innovation Center for Advanced Organic Chemical Materials, Hubei University, Wuhan 430062, People's Republic of China

<sup>‡</sup>Key Laboratory for Green Chemical Process of Ministry of Education and School of Chemistry and Environmental Engineering, Wuhan Institute of Technology, Wuhan 430205, People's Republic of China

<sup>§</sup>Key Laboratory for Advanced Materials and Institute of Fine Chemicals, East China University of Science and Technology, Shanghai 200237, People's Republic of China

## S Supporting Information

**ABSTRACT:** Nitroxyl (HNO) is a derivative of nitric oxide (NO) that plays an essential role in various biological and pharmacological events. Until now, the in situ trapping and specific detection of HNO in living samples is still challenging. In this project, we fabricated a novel BODIPY-based micellar nanoprobe for monitoring nitroxyl in vitro and in vivo in ratiometric mode in aqueous solution. The probe (P-BODIPY-N) contains an asymmetrical BODIPY dye for fluorescent signaling and a diphenylphosphinobenzoyl as the trigger moiety; then we encapsulated P-BODIPY-N into the hydrophobic interior of an amphiphilic copolymer (mPEG-DSPE) and prepared a novel BODIPY-based micellar nanoprobe: NP-BODIPY-N. As far as we know, this probe is the first reported ratiometric fluorescent nanoprobe for HNO, which exhibits ultrasensitivity, high selectivity, and good biocompatibility. Above all, this nanoprobe shows favorable cellular uptake and was successfully used to detect intracellular HNO released by Angeli's salt in living cells and zebrafish larvae. These results indicate that our newly designed nanoprobe will provide a promising tool for the studies of HNO in living system.



Nitroxyl (HNO), a one-electron reduced and protonated derivative of nitric oxide, plays a crucial role in many physiological and pathological processes and has attracted great interest in the past decades.<sup>1</sup> Several medical studies have demonstrated that HNO could exacerbate ischemia-related injury and induce vasorelaxation and could also treat heart failure and oxidize protein thiols to cause inhibition of aldehyde dehydrogenase and so on.<sup>2–4</sup> Thus, developing reliable analytical methods capable of monitoring biological nitroxyl is of great importance for therapeutic interventions. Nevertheless, HNO is a reactive molecule with poor stability in solutions or biological relevant samples,<sup>5</sup> which makes the detection of HNO full of challenges.

Until now, several analytical methods have been developed for the detection of HNO, such as electrochemical analysis, HPLC, NMR, mass spectrometry, and colorimetry.<sup>6–9</sup> Compared with these conventional methods, fluorescent probe is a powerful tool that has attracted extensive attention due to its ultrasensitivity, noninvasion detection, and the ability to real-time image the targets of interest in vitro and in vivo.<sup>10–22</sup> To date, several fluorescent probes have been developed to monitoring HNO, based on the reduction of Cu(II) to Cu(I),<sup>23–25</sup> or nitroxide to hydroxylamine.<sup>26</sup> However, these probes tend to be disturbed by abundant biological reductants, such as GSH and

ascorbate in living systems. Recently, various fluorescent probes have been developed to discriminate HNO from other biological reductants based on the reaction between HNO and triarylphosphine.<sup>27–33</sup> Despite advances in the development of anti-interference, this kind of new probe has shortcomings associated with poor water-solubility that is partly attributed to the phenyl structure in recognition moiety. As we all know, water solubility is a critical requirement for an ideal reaction-based fluorescent probe because numerous metabolic processes need to be proceeded in aqueous system. Nevertheless, few works have been done to solve this problem until now. Moreover, most of the above-mentioned fluorescent probes respond to HNO via fluorescence turn-on mode, which is susceptible to complex experimental conditions and inconvenient for quantitative analysis. Therefore, a ratiometric fluorescent probe that can overcome aforementioned disadvantages is urgently needed.

Boron dipyrromethene (BODIPY) derivatives are commonly used fluorophores sensitive to electronic effect. Our previous

Received: November 20, 2017

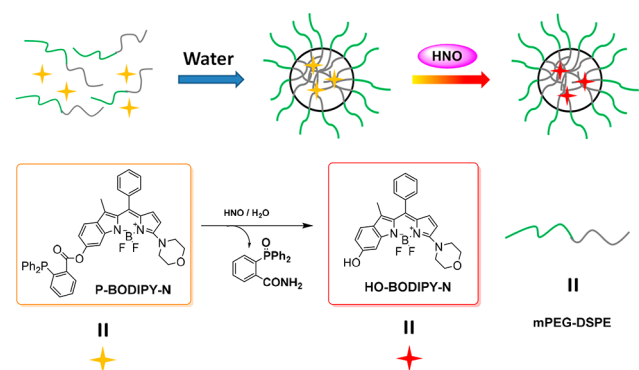
Accepted: January 15, 2018

Published: January 15, 2018

work has demonstrated that a change in electron-donating nature of the substituent on monochlorinated BODIPY could cause significant changes in fluorescence.<sup>34,35</sup> On the basis of these facts, a metal-free fluorogenic probe responded to HNO in ratiometric mode was developed. A monochlorinated BODIPY dye was chosen as the fluorophore with 2-(diphenylphosphino)benzoate as the recognition moiety. After conjugating morpholine to BODIPY dye and employing the nitrogen atom to improve the electron-donating ability, our newly designed probe P-BODIPY-N realized the detection of HNO in ratiometric mode. In the experiments, P-BODIPY-N shows very poor water-solubility, like some previous work reported.<sup>27–33</sup> Therefore, it cannot serve as the ideal responsive probe for HNO.

Recently, polymer encapsulated organic nanoparticles with several significant advantages, such as superb photo- and physical stability, potential biodegradability and good biocompatibility, and so on,<sup>36–39</sup> have attracted great interest in biochemistry. In this regard, we considered encapsulating the poor water-soluble fluorescent probe (P-BODIPY-N) into the hydrophobic interior of the micelles by self-assembly of amphiphilic copolymer mPEG-DSPE (1,2-dimyristoyl-*sn*-glycero-3-phospho-ethanolamine-*N*-(methoxy(polyethylene glycol)-2000)) and prepared a micellar aggregate nanoprobe.<sup>40–43</sup> As shown in Scheme 1, the

**Scheme 1. Chemical Structure of P-BODIPY-N and Formation of Micellar Nanoprobe (NP-BODIPY-N) for Recognition of HNO**



hydrophilic moieties of mPEG-DSPE were distributed in the exterior of the cluster. These features can dramatically improve the water-solubility of the nanoprobe. In this way, the unique self-assembled micellar nanoprobe (NP-BODIPY-N), can be well dispersed in water. Moreover, the nanoprobe showed fast response, ultrasensitivity, and favorable cellular uptake, which can trap endogenous HNO in living samples. As far as we know, our newly designed self-assembled micelle nanoprobe, NP-BODIPY-N, is the first reported ratiometric fluorescent nanoprobe for HNO with numerous advantages.

## EXPERIMENTAL SECTION

**Materials and Instruments.** Unless otherwise noted, all reagents and solvents were purchased from commercial suppliers and used without further purification. Distilled water was used in the experiment after passing through a water ultra-purification system. Silica gel (200–300 mesh) was used for flash column chromatography. <sup>1</sup>H and <sup>13</sup>C NMR spectra were recorded on a Bruker AV-600 spectrometer. Mass spectra were measured on Agilent 1100 Series. UV–vis absorption spectra were obtained on a SHIMADZU UV-1800 spectrophotometer. Fluorescence spectra were measured by Agilent Cary Eclipse Fluorescence spectrophotometer.

**Synthesis of HO-BODIPY-S and HO-BODIPY-N.** The two BODIPY-based fluorophore were synthesized following the previous method.<sup>34</sup>

**Synthesis of P-BODIPY-S.** HO-BODIPY-S (50 mg, 0.1063 mmol), 2-(diphenylphosphino) benzoic acid (39.2 mg, 0.1281 mmol), DPTS (31.2 mg, 0.1063 mmol), and DIPC (13.4 mg, 0.1063 mmol) were dissolved in dichloromethane. The reaction was stirred at room temperature for 5 h under argon. After the reaction completed, the mixture was diluted with CH<sub>2</sub>Cl<sub>2</sub> and washed with water for 3×. The organic layer was dried with anhydrous Na<sub>2</sub>SO<sub>4</sub>, and the solvent was then evaporated in vacuo. The residual was purified by silica gel chromatography with CH<sub>2</sub>Cl<sub>2</sub>/PE to get the target P-BODIPY-S (40 mg, 0.0531 mmol), and the yield was 50%. <sup>1</sup>H NMR (*d*<sub>6</sub>-DMSO, 600 MHz): δ 8.07 (q, 1H), δ 7.83 (t, 1H), δ 7.73 (t, 2H), δ 7.66–7.60 (m, 12H), δ 7.57–7.51 (m, 5H), δ 7.42–7.39 (m, 4H), δ 6.85 (q, 1H), δ 6.79 (d, 1H), δ 6.02 (d, 1H), δ 2.40 (s, 3H), δ 1.73 (s, 3H); HRMS (ESI) Calcd for C<sub>46</sub>H<sub>34</sub>BF<sub>2</sub>N<sub>2</sub>O<sub>2</sub>PS, 757.2182; Found, 757.2162 [M – H]<sup>–</sup> (Figure S1).

**Synthesis of P-BODIPY-N.** P-BODIPY-N was synthesized followed the same procedure of P-BODIPY-S, and the synthesis yield was about 40%. <sup>1</sup>H NMR (*d*<sub>6</sub>-DMSO, 600 MHz): δ 8.26 (q, 1H), δ 7.59 (t, 2H), δ 7.54 (d, 2H), δ 7.42–7.38 (m, 10H), δ 7.22–7.19 (m, 5H), δ 6.98 (d, 1H), δ 6.93 (d, 1H), δ 6.77 (d, 1H), δ 6.56 (d, 1H), δ 4.10 (s, 1H), δ 3.82 (s, 1H); <sup>13</sup>C NMR (*d*<sub>6</sub>-DMSO, 150 MHz): δ 165.16, 161.90, 147.88, 140.40, 140.05, 139.87, 139.20, 137.21, 137.14, 135.30, 134.49, 133.76, 133.57, 133.50, 133.43, 133.37, 132.74, 132.04, 131.06, 129.92, 129.09, 128.94, 128.88, 128.84, 128.75, 128.70, 128.52, 119.97, 118.61, 118.32, 114.06, 106.18, 66.26, 50.75, 10.24; HRMS (ESI) Calcd for C<sub>43</sub>H<sub>35</sub>BF<sub>2</sub>N<sub>3</sub>O<sub>3</sub>P, 720.2519; Found, 720.2506 [M – H]<sup>–</sup> (Figure S2).

**Preparation of NP-BODIPY-N.** mPEG-DSPE (11 mg) was poured into a vial containing 1 mL of distilled–deionized water under vigorous sonication for 20 min, then P-BODIPY-N (0.11 mg) was rapidly added into the mixture and kept continuous sonication for another 20 min. After that, the solution was filtered through a 0.22 μm polyvinylidene fluoride (PVDF) syringe driven filter, and further dialyzed with distilled–deionized water for 12 h to remove other chemicals. In these process, the nanoprobe stock solution was prepared, the concentration of NP-BODIPY-N in PBS buffer solution was determined according to the UV–vis standard absorption curve.

**General Optical Measurements.** For absorption and fluorescence measurements, stock solution of P-BODIPY-S and P-BODIPY-N in CH<sub>3</sub>CN were first prepared (5.0 mM) and stored at –20 °C before use. The stock solution were then diluted with acetonitrile/PBS buffer solution (1:9, v/v, pH = 7.4) to the desired concentration for measurements.

**Determination of Quantum Yield.** According to the reported method,<sup>44,45</sup> the fluorescence quantum yields in this work were determined with rhodamine 6G as reference. More specifically, using rhodamine 6G (Φ = 0.94, ethanol) as reference, the probes were prepared in phosphate-buffered saline (PBS, 0.02 M, pH = 7.4) buffer solution and diluted to appropriate concentration to make their absorption less than 0.05. Then, the absorbance and the corresponding emission integral area were measured at this concentration. After determined the refractive index of the samples in different solvents by an Abbe's refractometer, the quantum yields were calculated with the following equation.

$$\Phi_s = \frac{F_s \cdot A_c}{F_c \cdot A_s} \Phi_c$$

where the  $\Phi_s$  and  $\Phi_c$  are the fluorescence quantum yield of the test and standard sample;  $F_s$  and  $F_c$  are the integrated fluorescence intensity of the test and standard sample;  $A_s$  and  $A_c$  are the absorbance at the excitation wavelength of the test and standard sample, respectively.

**Selectivity Evaluation.** To study the interference, the various testing analytes stock solution (Hcy,  $\text{Na}_2\text{S}$ , HA,  $\text{FeCl}_3$ ,  $\text{NaClO}$ , AA,  $\text{H}_2\text{O}_2$ ,  $\text{NO}_3^-$ ,  $\text{NO}_2^-$ , GSNO, NOC7, NOR1,  $\text{ONOO}^-$ , SNAP) were prepared at 200  $\mu\text{M}$ , FBS: 10% (v/v), and GSH, Cys were prepared at 5 mM and 1 mM in twice distilled water, respectively. NP-BODIPY-N (10  $\mu\text{M}$ ) incubated with each analyte for 20 min in physiological conditions. Then the fluorescence spectra were measured.

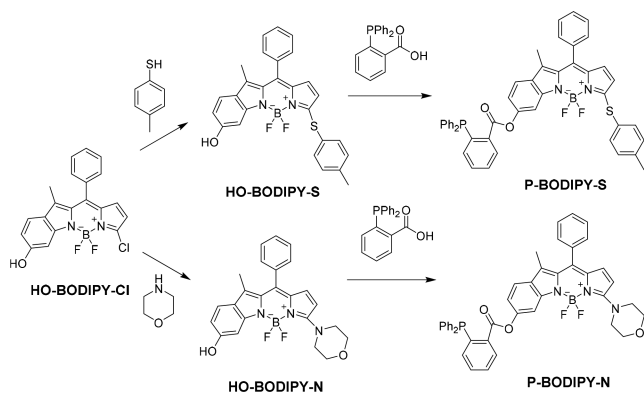
**Cell Cultures and Imaging.** HepG2 cells were cultured in Dulbecco's modified Eagle's medium (DMEM) supplemented with 10% fetal bovine serum and penicillin–streptomycin (0.5  $\text{U}\cdot\text{mL}^{-1}$  of penicillin and 0.5  $\text{g}\cdot\text{mL}^{-1}$  streptomycin) on a cell culture flask at 37 °C in an atmosphere of air with 5%  $\text{CO}_2$  and constant humidity. Each cell line was seeded in a 6-well plate for 24 h. The cells were initially incubated with NP-BODIPY-N (10  $\mu\text{M}$ ) in culture medium for 30 min at 37 °C. After washing three times with PBS to remove the remaining NP-BODIPY-N, the HepG2 cells were incubated in the absence or presence of AS (50  $\mu\text{M}$ ) in culture medium for another 20 min at 37 °C. the imaging was carried out using inverted fluorescence microscopy (Olympus IX71, Japan).

**Imaging of Zebrafish.** The 3–7 days old zebrafishes postfertilization were purchased from Eze-Rinka Company (Nanjing, China). The zebrafishes were cultured in 5 mL of embryo medium supplemented with 1-phenyl-2-thiourea (PTU) in 6-well plates for 24 h at 30 °C. Zebrafishes were divided into two groups and both incubated with NP-BODIPY-N (10  $\mu\text{M}$ ) for 12 h. One group as the control group and the other group further treated with AS (50  $\mu\text{M}$ ) for another 20 min. All samples were washed three times to remove the remaining NP-BODIPY-N before imaging. And the fluorescence images were acquired with stereo microscopy (Olympus SZX16, Japan).

## RESULTS AND DISCUSSION

**Synthesis of P-BODIPY-S and P-BODIPY-N.** The two BODIPY-based fluorescence probes P-BODIPY-S and P-BODIPY-N were synthesized in two steps via a nucleophilic aromatic substitution ( $\text{S}_{\text{N}}\text{Ar}$ ) and followed by an esterification as shown in Scheme 2. The purity and structure were confirmed by NMR and HRMS.

**Scheme 2.** Synthesis Procedure of P-BODIPY-S and P-BODIPY-N



**Probe Characterization.** First, the photophysical properties of P-BODIPY-S were assessed in the absence and presence of HNO (in all experiments, Angeli's salt (AS) was employed as the HNO source) in acetonitrile/PBS buffer solution (1:9, v/v, pH = 7.4). Here, acetonitrile was chosen as the cosolvent to improve the aqueous solubility of the probe. As shown in Figure S3, the free P-BODIPY-S showed relatively weak fluorescence ( $\Phi = 0.001$ ), while a dramatic fluorescence enhancement at 608 nm was observed after its exposure to HNO. It indicates that the probe showed good response to HNO in a turn-on mode. Though the BODIPY-based fluorescent probe, P-BODIPY-S, can fulfill the purpose of monitoring HNO, it cannot meet our requirements to detect HNO in ratiometric mode. On the basis of these facts, we specially fine-tuned the electronic effects of the probe, and further developed P-BODIPY-N that possesses a stronger electron-donating moiety. The spectral properties were investigated in the same physiological conditions. As illustrated in Figure 1, P-BODIPY-N exhibited a strong

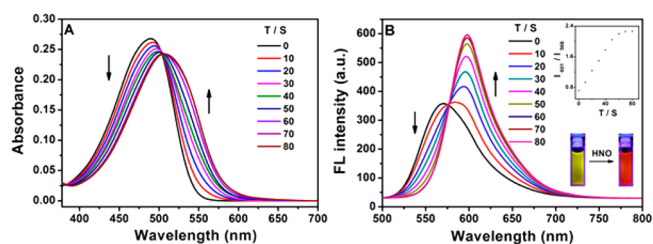


**Figure 1.** Time-dependent optical changes in absorption (A) and emission (B) of P-BODIPY-N (10  $\mu\text{M}$ ) in the presence of AS (50  $\mu\text{M}$ ) in acetonitrile/PBS buffer solution (1:9, v/v, pH = 7.4) at 37 °C. ( $\lambda_{\text{ex}} = 480 \text{ nm}$ ). Inset: Emission ratio ( $I_{601}/I_{568}$ ) changes of P-BODIPY-N after exposure to HNO and the photo of P-BODIPY-N solution before and after addition of AS.

absorption band at 491 nm and a remarkable emission peak at 568 nm ( $\Phi = 0.021$ ). After addition of 5 equiv AS, the absorption band at 491 nm was dramatically red-shifted to 510 nm. While in the fluorescence spectra, the emission band of P-BODIPY-N at 568 nm decreased rapidly and accompanied by a sharp fluorescence enhancement at 601 nm, and the fluorescence intensity ratio ( $I_{601}/I_{568}$ , Figure S4) reached plateau within 80 s. Impressively, this obvious ratio change can be dramatically suppressed by GSH (Figure S5), a HNO scavenger,<sup>27</sup> in a dose-dependent manner. The results indicated that the ratiometric signal was specifically induced by HNO activity. To get further insight into the sensing process, HPLC analysis and HRMS characterization were also carried out. As illustrated in Figure S6, pure P-BODIPY-N and HO-BODIPY-N both gave a unique narrow peak with retention time at about 12.433 and 3.907 min, respectively. After treating P-BODIPY-N with HNO for several minutes, a new narrow peak with retention time at about 3.920 min was clearly observed and corresponded well with HO-BODIPY-N. In addition, the final product of P-BODIPY-N + HNO was further conformed by HRMS analysis (Figure S6E). All these results demonstrated that P-BODIPY-N could successfully detect HNO in ratiometric mode.

Although P-BODIPY-N realized the detection of HNO in ratiometric mode and overcome several defects, the water-solubility was still hard to be solved (Figure S7A), like some previous works reported.<sup>27–33</sup> Thus, we considered encapsulating P-BODIPY-N into the core of a micelle via the self-assembly of the amphiphilic copolymer mPEG-DSPE and prepared a

unique water-dispersible nanoprobe (NP-BODIPY-N). Briefly, P-BODIPY-N was entrapped into the hydrophobic interiors of the nanoscale micelle, and the hydrophilic unit of mPEG-DSPE was distributed in the exterior of the cluster and dramatically improved the water-solubility (Figure S7B). The XPS results confirmed that P-BODIPY-N was encapsulated into the micelle (Figure S8). Moreover, the average hydrodynamic size of these micelles (NP-BODIPY-N) was about  $100 \pm 10$  nm measured by TEM (transmission electron microscopy) and DLS (dynamic light scattering; Figure 2E,F).

With the unique nanoprobe in hand, we first investigated its stability in physiological conditions. When the fluorescence intensity ratio ( $I_{601}/I_{568}$ ) was chosen as the detection signal, the nanoprobe showed excellent fluorescence stability in aqueous solution (Figure S9A). Furthermore, to confirm the micellar nanoprobe was neither aggregated nor precipitated in aqueous solution, the samples were also evaluated by DLS for several days. Impressively, the micellar nanoprobe showed minimal changes (Figure S9B). These results indicated the excellent stability of NP-BODIPY-N. On the bases of these facts, the responsive features of NP-BODIPY-N to HNO were subsequently investigated in PBS buffer solution (pH = 7.4). Compared with the free dye P-BODIPY-N, which need the help of acetonitrile to dissolve in aqueous solution, NP-BODIPY-N showed excellent water-solubility (Figure S7B). As illustrated in Figure 2, NP-BODIPY-N retained its promising optical response to HNO,

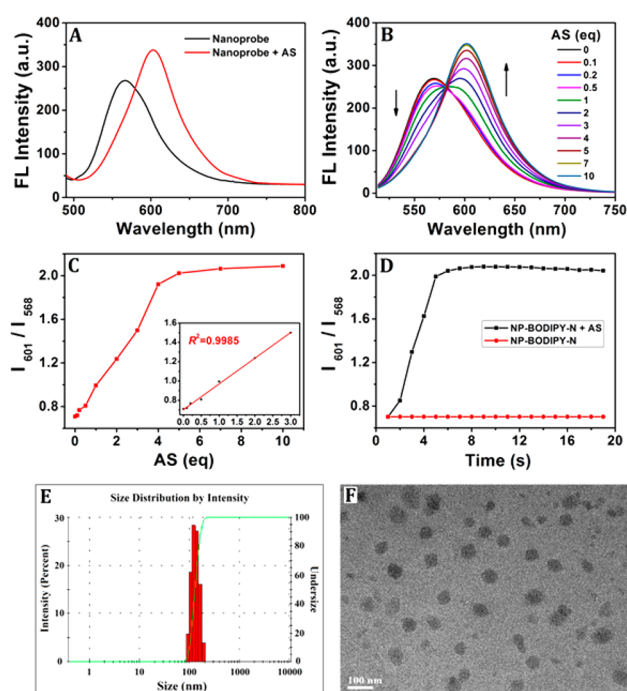


**Figure 2.** (A) Fluorescence spectra of NP-BODIPY-N ( $10 \mu\text{M}$ ) in the absence and presence of AS ( $50 \mu\text{M}$ ) in PBS buffer solution (pH = 7.4). (B) Fluorescence spectra of NP-BODIPY-N ( $10 \mu\text{M}$ ) after 10 min upon treatment with increasing concentration of AS (0– $100 \mu\text{M}$ ). (C) Fluorescence intensity ratio ( $I_{601}/I_{568}$ ) changes of NP-BODIPY-N upon exposure to HNO. Inset: The ratio ( $I_{601}/I_{568}$ ) as a function of AS concentration. (D) Fluorescence intensity ratio ( $I_{601}/I_{568}$ ) as a function of time. ( $\lambda_{\text{ex}} = 480$  nm). (E) Hydrodynamic size of NP-BODIPY-N in aqueous solution measured by dynamic light scattering (DLS). (F) TEM imaging of NP-BODIPY-N. Note: The average hydrodynamic size of these self-assembled micelles nanoprobe is about 100 nm as measure by DLS and TEM.

after the addition of 5 equiv AS to the NP-BODIPY-N solution. The emission at 568 nm sharply decreased and a new band at 601 nm was observed (Figure S10), which showed an  $I_{601}/I_{568}$  variation from 0.68 to 2.08, and indicated an efficient ratiometric response to HNO. It is worth noticing that the fluorescence signal change could be observed in a few seconds (Figure 2A). This fast response character was highly suitable for real-time images of HNO-related biological processes. In addition, the fluorescence ratio  $I_{601}/I_{568}$  was linearly proportional to the AS concentration in the range of 0–3 equiv (Figure 2C), and the detection limit was calculated to be 8.82 nM for HNO (based on  $3\sigma/\text{slope}$ ), which was much lower than the limits of previous works,<sup>27–33</sup> indicating NP-BODIPY-N is anticipated to trap endogenous generation of HNO in living samples.

#### pH Effect on the Response of NP-BODIPY-N to HNO.

As the pH value of the cellular compartments, a number of reported probes face pH dependency issue, hampering their application in biological system. Therefore, developing novel probe that can well overcome the limitation is necessary. We herein, evaluated the pH effects on the ratiometric response of NP-BODIPY-N to HNO (Figure S11). Fortunately, not only the micellar nanoprobe itself, but also the response properties showed slight influence over the range of pH 5.0 to 9.0. These results indicated that the nanoprobe has good stability and sensitive response to HNO in a wide pH value.

#### Selectivity of NP-BODIPY-N.

To examine the selectivity, the reactivity of the micellar nanoprobe toward other biological analytes was evaluated by measuring its fluorescence ratio value at  $I_{601}/I_{568}$  in PBS buffer solution. As illustrated in Figure 3,

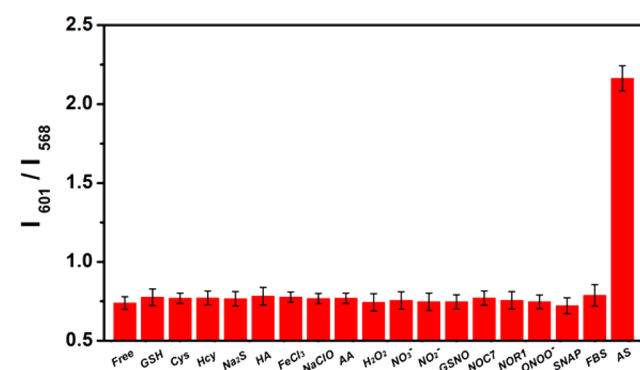


**Figure 3.** Fluorescence responses of the NP-BODIPY-N ( $10 \mu\text{M}$ ) in the presence of AS and various relevant analytes (GSH: 5 mM, Cys: 1 mM, 10% FBS, others:  $200 \mu\text{M}$ ) in PBS buffer solution (50 mM, pH = 7.4) at  $37^\circ\text{C}$  for 20 min,  $\lambda_{\text{ex}} = 480$  nm. Data represent average values of three independent experiments.

only AS can trigger a remarkable enhancement in the fluorescence intensity ratio value, while other analytes (such as reactive sulfur (RSS), oxygen (ROS), and nitrogen species (RNS)) gave negligible response. These results confirmed that NP-BODIPY-N has an excellent selectivity toward HNO over other biological related species.

**Cellular Imaging.** After investigating the responsive behavior of NP-BODIPY-N toward HNO in vitro, we attempted to examine whether the nanoprobe could be suitable for imaging of HNO in living cells in ratiometric mode. The cytotoxicity of free NP-BODIPY-N was initially evaluated using typical MTT assays, HepG2 cells was chosen as the cell model, and the results revealed that NP-BODIPY-N coexisted well with living cancer cells.

Since the probe shows good biocompatibility, we then investigate its performance in HepG2 cells. After the cells incubated with NP-BODIPY-N for 30 min, as shown in Figure 4, an

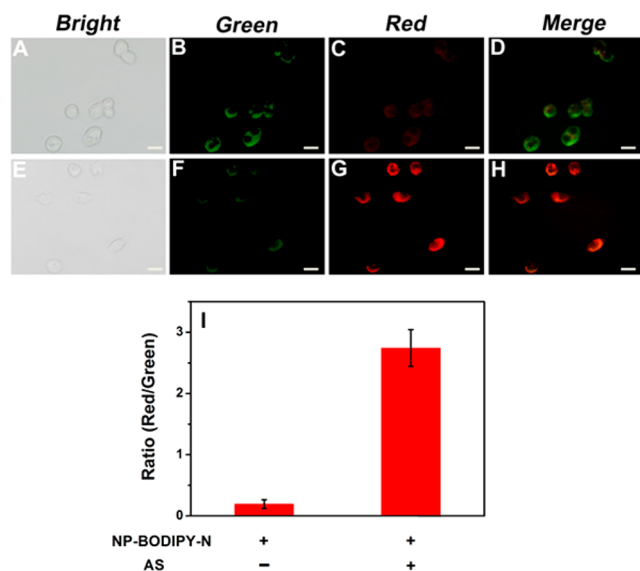


**Figure 4.** Fluorescent imaging of HepG2 cells incubated with NP-BODIPY-N ( $10 \mu\text{M}$ ) for 30 min (A–D), and then with AS ( $50 \mu\text{M}$ ) for another 10 min (E–H). (A, E) bright field imaging, (B, F) green channel (510–550 nm), (C, G) red channel (590–650 nm), (D, H) ratio/merge image generated from red channel to green channel, (I) average intensity ratios from red channel to green channel. Data represent mean standard error ( $n = 3$ ), scale bar =  $20 \mu\text{m}$ .

intense intracellular fluorescence in green channel and relatively weak fluorescence in red channel were observed. The ratio of the two emissions from red channel to green channel was about 0.19 (Figure 4I), which indicated that NP-BODIPY-N is cell-permeable. While after the addition of  $50 \mu\text{M}$  AS, and a further incubation for 10 min, the intracellular fluorescence was declined in green channel and significantly enhanced in red channel. The ratio (red channel to green channel) increased to about 2.74 (Figure 4I). These results suggested that NP-BODIPY-N could be used for the ratiometric fluorescence image of HNO in living cells.

**In Vivo Imaging of Zebrafish.** To further explore the application of NP-BODIPY-N, fluorescence imaging in zebrafish models was conducted. In these experiments, NP-BODIPY-N ( $10 \mu\text{M}$ ) was first incubated with zebrafish larvae for 12 h, and a bright fluorescence in green channel was observed in digestive system of the zebrafish larvae, while a relatively weak fluorescence signal was collected in red channel. The ratio of the two emissions from red channel to green channel was about 0.23. While after treated with AS ( $50 \mu\text{M}$ ) for another 20 min, the fluorescence signal gave a subversive change, the red channel increased and the green channel decreased obviously. The emission ratio (red channel/green channel) increased nearly 10-fold from 0.23 to 2.25 (Figure 5). These results indicated that NP-BODIPY-N was organism-permeable and extraordinarily sensitive to track trace amount of endogenous HNO in living samples.

## CONCLUSION

In summary, we reported the design and biological evaluation of a novel first reported ratiometric fluorescent nanoprobe (NP-BODIPY-N) for the detection of HNO both in vitro and

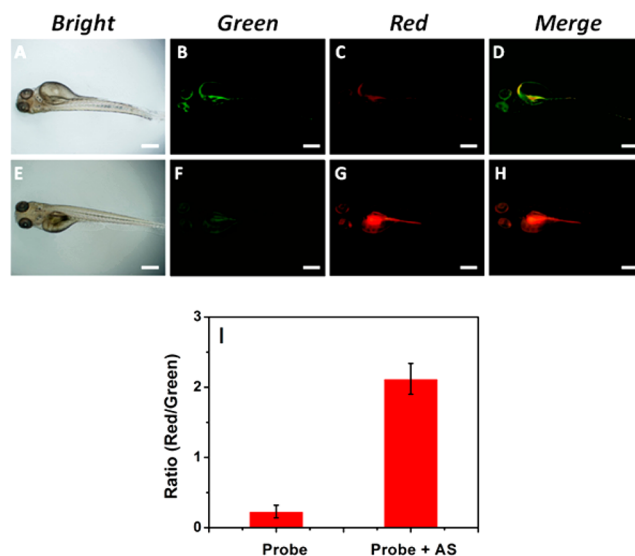


**Figure 5.** Fluorescent imaging of zebrafish larvae incubated with NP-BODIPY-N ( $10 \mu\text{M}$ ) for 12 h (A–D) and further treated with AS ( $50 \mu\text{M}$ ) for another 20 min (E–H); (A, E) bright field imaging, (B, F) green channel (510–550 nm), (C, G) red channel (590–650 nm), (D, H) ratio/merge image generated from red channel to green channel, (I) average intensity ratios from red channel to green channel. Data represent mean standard error ( $n = 3$ ), scale bar =  $20 \mu\text{m}$ .

in vivo. The metal-free nanoprobe realized the highly chemoselective detection of HNO in ratiometric mode in aqueous solution. Furthermore, the nanoprobe exhibited excellent stability, high selectivity and ultra sensitivity (the detection limit is as low as  $8.82 \text{ nM}$ ). Importantly, such a unique nanoprobe afforded favorable cellular uptake and was successfully used to detect HNO in living cells and further to capture endogenous HNO in zebrafish larvae. On the basis of these findings, we believe that NP-BODIPY-N will provide a promising tool for the studies of HNO in living systems.

## ASSOCIATED CONTENT

### Supporting Information

The Supporting Information is available free of charge on the ACS Publications website at DOI: 10.1021/acs.analchem.7b04787.

Additional information as noted in text (PDF).

## AUTHOR INFORMATION

### Corresponding Authors

\*E-mail: wangfyi@hubu.edu.cn.

\*E-mail: qisun@wit.edu.cn.

\*E-mail: zhaocchang@ecust.edu.cn.

### ORCID

Feiyi Wang: 0000-0003-2936-5276

Chunchang Zhao: 0000-0003-2952-7036

Wei-Hong Zhu: 0000-0001-9103-166X

### Notes

The authors declare no competing financial interest.

## ACKNOWLEDGMENTS

We gratefully acknowledge the financial support by the National Natural Science Foundation of China (21702053, 21676075), the Hubei Provincial Department of Education Project (Q20171013), and the Hubei Provincial Natural Science Foundation of China (2016CFB262, 2017CFB222).

## REFERENCES

- (1) Chen, X. Q.; Wang, F.; Hyun, J. Y.; Wei, T. W.; Qiang, J.; Ren, X. T.; Shin, I.; Yoon, J. *Chem. Soc. Rev.* **2016**, *45*, 2976–3016.
- (2) Xu, W.; Liu, L. Z. M.; Ahmed, L. M.; Charles, I. G. *Cell Res.* **2002**, *12*, 311–320.
- (3) Muenzel, T.; Feil, R.; Muelsch, A.; Lohmann, S. M.; Hofmann, F.; Walter, U. *Circulation* **2003**, *108*, 2172–2183.
- (4) DeMaster, E. G.; Redfern, B.; Nagasawa, H. T. *Biochem. Pharmacol.* **1998**, *55*, 2007–2015.
- (5) Shafirovich, V.; Lymar, S. V. *Proc. Natl. Acad. Sci. U. S. A.* **2002**, *99*, 7340–7345.
- (6) Suárez, S. A.; Bikiel, D. E.; Wetzler, D. E.; Martí, M. A.; Doctorovich, F. *Anal. Chem.* **2013**, *85*, 10262–10269.
- (7) Kitamura, N.; Hiraoka, T.; Tanaka, K.; Chujo, Y. *Bioorg. Med. Chem.* **2012**, *20*, 4668–4674.
- (8) Cline, M. R.; Tu, C.; Silverman, D. N.; Toscano, J. P. *Free Radical Biol. Med.* **2011**, *50*, 1274–1279.
- (9) Reisz, J. A.; Zink, C. N.; King, S. B. *J. Am. Chem. Soc.* **2011**, *133*, 11675–11685.
- (10) Zhao, J. Z.; Xu, K. J.; Yang, W. B.; Wang, Z. J.; Zhong, F. F. *Chem. Soc. Rev.* **2015**, *44*, 8904–8939.
- (11) Zhou, Z.; Wang, F. Y.; Yang, G. C.; Lu, C. F.; Nie, J. Q.; Chen, Z. X.; Ren, J.; Sun, Q.; Zhao, C. C.; Zhu, W. H. *Anal. Chem.* **2017**, *89*, 11576–11582.
- (12) Song, J. X.; Tang, X. Y.; Zhou, D. M.; Zhang, W. Q.; James, T. D.; He, X. P.; Tian, H. *Mater. Horiz.* **2017**, *4*, 431–436.
- (13) Gong, Q. Y.; Shi, W.; Li, L. H.; Ma, H. M. *Chem. Sci.* **2016**, *7*, 788–792.
- (14) Jia, X. T.; Chen, Q. Q.; Yang, Y. F.; Tang, Y.; Wang, R.; Xu, Y. F.; Zhu, W. P.; Qian, X. H. *J. Am. Chem. Soc.* **2016**, *138*, 10778–10781.
- (15) Tong, H. J.; Zheng, Y. J.; Zhou, L.; Li, X. M.; Qian, R.; Wang, R.; Zhao, J. H.; Lou, K. Y.; Wang, W. *Anal. Chem.* **2016**, *88*, 10816–10820.
- (16) Tong, J.; Wang, Y.; Mei, J.; Wang, J.; Qin, A.; Sun, J. Z.; Tang, B. Z. *Chem. - Eur. J.* **2014**, *20*, 4661–4670.
- (17) Wang, Y. F.; Liu, C. X.; Wang, T. L.; Hong, T. T.; Su, H. M.; Yu, S. Y.; Song, H. W.; Liu, S. M.; Zhou, X.; Mao, W. X.; Zhou, X. *Anal. Chem.* **2016**, *88*, 3348–3353.
- (18) Shen, B. X.; Qian, Y.; Qi, Z. Q.; Lu, C. G.; Sun, Q.; Xia, X.; Cui, Y. P. *J. Mater. Chem. B* **2017**, *5*, 5854–5861.
- (19) Fan, J. L.; Hu, M. M.; Zhan, P.; Peng, X. J. *Chem. Soc. Rev.* **2013**, *42*, 29–43.
- (20) Montoya, L. A.; Pluth, M. D. *Anal. Chem.* **2014**, *86*, 6032–6039.
- (21) Wang, J. Y.; Xue, J.; Yan, Z. H.; Zhang, S. C.; Qiao, J.; Zhang, X. R. *Angew. Chem., Int. Ed.* **2017**, *56*, 14928–14932.
- (22) Lee, M. H.; Kim, J. S.; Sessler, J. L. *Chem. Soc. Rev.* **2015**, *44*, 4185–4191.
- (23) Apfel, U. P.; Buccella, D.; Wilson, J. J.; Lippard, S. J. *Inorg. Chem.* **2013**, *52*, 3285–3294.
- (24) Wrobel, A. T.; Johnstone, T. C.; Liang, A. D.; Lippard, S. J.; Rivera-Fuentes, P. *J. Am. Chem. Soc.* **2014**, *136*, 4697–4705.
- (25) Zhou, Y.; Liu, K.; Li, J. Y.; Fang, Y.; Zhao, T. C.; Yao, C. *Org. Lett.* **2011**, *13*, 1290–1293.
- (26) Cline, M. R.; Toscano, J. P. *J. Phys. Org. Chem.* **2011**, *24*, 993–998.
- (27) Kawai, K.; Ieda, N.; Aizawa, K.; Suzuki, T.; Miyata, N.; Nakagawa, H. *J. Am. Chem. Soc.* **2013**, *135*, 12690–12696.
- (28) Zheng, K. B.; Lin, W. Y.; Cheng, D.; Chen, H.; Liu, Y.; Liu, K. Y. *Chem. Commun.* **2015**, *51*, 5754–5757.
- (29) Mao, G. J.; Zhang, X. B.; Shi, X. L.; Liu, H. W.; Wu, Y. X.; Zhou, L. Y.; Tan, W. H.; Yu, R. Q. *Chem. Commun.* **2014**, *50*, 5790–5792.
- (30) Sunwoo, K.; Bobba, K. N.; Lim, J.; Park, T.; Podder, A.; Heo, J. S.; Lee, S. G.; Bhuniya, S.; Kim, J. S. *Chem. Commun.* **2017**, *53*, 1723–1726.
- (31) Zhu, X. Y.; Xiong, M. Y.; Liu, H. W.; Mao, G. J.; Zhou, L. Y.; Zhang, J.; Hu, X. X.; Zhang, X. B.; Tan, W. H. *Chem. Commun.* **2016**, *52*, 733–736.
- (32) Zhou, Y. B.; Zhang, X. F.; Yang, S.; Li, Y.; Qing, Z. H.; Zheng, J.; Li, J. S.; Yang, R. H. *Anal. Chem.* **2017**, *89*, 4587–4594.
- (33) Ren, M. G.; Deng, B. B.; Zhou, K.; Wang, J. Y.; Kong, X. Q.; Lin, W. Y. *J. Mater. Chem. B* **2017**, *5*, 1954–1961.
- (34) Wang, F. Y.; Zhou, L.; Zhao, C. C.; Wang, R.; Fei, Q.; Luo, S. H.; Guo, Z. Q.; Tian, H.; Zhu, W. H. *Chem. Sci.* **2015**, *6*, 2584–2589.
- (35) Wang, F. Y.; Zhu, Y.; Zhou, L.; Pan, L.; Cui, Z. F.; Fei, Q.; Luo, S. H.; Pan, D.; Huang, Q.; Wang, R.; Zhao, C. C.; Tian, H.; Fan, C. H. *Angew. Chem., Int. Ed.* **2015**, *54*, 7349–7353.
- (36) Li, K.; Liu, B. *Chem. Soc. Rev.* **2014**, *43*, 6570–6597.
- (37) Li, Y. S.; Shao, A. D.; Wang, Y.; Mei, J.; Niu, D. C.; Gu, J. L.; Shi, P.; Zhu, W. H.; Tian, H.; Shi, J. L. *Adv. Mater.* **2016**, *28*, 3187–3193.
- (38) Zhao, Y. W.; Zou, C. L.; Zhao, H. K.; Zhao, L. N. *Sci. China: Chem.* **2016**, *59*, 255–263.
- (39) Kotova, O.; Comby, S.; Lincheneau, C.; Gunnlaugsson, T. *Chem. Sci.* **2017**, *8*, 3419–3426.
- (40) Swaminathan, S.; Garcia-Amorós, J.; Fraix, A.; Kandoth, N.; Sortino, S.; Raymo, F. M. *Chem. Soc. Rev.* **2014**, *43*, 4167–4178.
- (41) Zhao, C. C.; Zhang, X. L.; Li, K. B.; Zhu, S. J.; Guo, Z. Q.; Zhang, L. L.; Wang, F. Y.; Fei, Q.; Luo, S. H.; Shi, P.; Tian, H.; Zhu, W. H. *J. Am. Chem. Soc.* **2015**, *137*, 8490–8498.
- (42) Hu, J. M.; Liu, S. Y. *Acc. Chem. Res.* **2014**, *47*, 2084–2095.
- (43) Swaminathan, S.; Fowley, C.; McCaughan, B.; Cusido, J.; Callan, J. F.; Raymo, F. M. *J. Am. Chem. Soc.* **2014**, *136*, 7907–7913.
- (44) Sun, Q.; Yang, S. H.; Wu, L.; Dong, Q. J.; Yang, W. C.; Yang, G. F. *Anal. Chem.* **2016**, *88*, 6084–6091.
- (45) Li, J.; Zhang, C. F.; Yang, S. H.; Yang, W. C.; Yang, G. F. *Anal. Chem.* **2014**, *86*, 3037–3042.